

# Pseudoscalar current and covariance with the light-front approach

J. Leão

*Laboratório de Física Teórica e Computacional - LFTC  
Universidade Cruzeiro do Sul and Universidade Cidade de São Paulo  
01506-000 São Paulo, Brazil, and Instituto Federal de São Paulo  
Avenida Bahia, Caraguatatuba 11665-071 São Paulo, Brazil*

J. P. B. C. de Melo

*Laboratório de Física Teórica e Computacional - LFTC, Universidade Cruzeiro do Sul  
and Universidade Cidade de São Paulo 01506-000 São Paulo, Brazil*

Received 24 February 2023; accepted 4 June 2023

Quantum Field Theory (QFT) is used to describe the physics of particles in terms of their fundamental constituents. The Light-Front Field Theory (LFFT), introduced by Paul Dirac in 1949 [1], is an alternative approach to solve some of the problems that arise in quantum field theory. The LFFT is similar to the Equal Time Quantum Field Theory (EQT), however, some particularities are not, such as the loss of covariance in the light-front. Pion electromagnetic form factor is studied in this work at lower and higher momentum transfer regions to explore the constituent quark models and the differences among these and other models. The electromagnetic current is calculated with both the “plus” and “minus” components in the light-front approach. The results are compared with other models, as well as with experimental data.

*Keywords:* Pion; light-front; quark model; electromagnetic current; electromagnetic form factor.

DOI: <https://doi.org/10.31349/RevMexFis.69.060801>

## 1. Introduction

Quantum chromodynamics (QCD), the theory of strong interactions, consists in the study of one of the four fundamental interactions in the standard model. One of the most important questions in QCD, not yet resolved, is in regard of the non-perturbative regime. To address this particular issue is not straightforward, although lattice QCD has been progressing and thus promising advances are expected.

Even with some relativistic constituent quark models, it is possible to study hadron physics in non-perturbative regions in an efficient manner with the quark and gluon degrees of freedom [2]. Before the advent of QCD, the pion, the lightest mass in hadrons regarded as the quark-antiquark bound state, has provided the long-range attractive part of the nucleon-nucleon interaction [3]. Amongst other approaches, the light-front aims to consistently describe the pion (hadron) bound state involving both the higher and lower momentum transfer regions. Hence, the light-front quantization has been used to compute the hadronic bound state wave functions [2,4]. The advantage of the light-front approach compared to the instant form is its simplicity [5].

In the light-front approach, the bound state wave functions are defined in the hypersurface,  $x^+ = x^0 + x^3 = 0$ , and are covariant under kinematical front-form boosts, because of the Fock-state decomposition stability [6]. Due to the simplicity in handling the wave functions and calculating observables, the light-front constituent quark model (LFCQM) has received a lot of attention in the past [7, 8]. The LFCQMs achieved impressive success in describing the electromag-

netic properties of hadrons, in particular those of the pseudoscalar and spin-1/2 particles [9-30], as well as spin-1 vector particles [31-38].

The extraction of the electromagnetic form factor with the light-front approach depends on the electromagnetic current’s component adopted, due to problems related with the rotational symmetry breaking and the zero modes, namely, a non-valence contribution to the electromagnetic current’s matrix elements [31,32,39,40].

It is discussed in Refs. [31,32,41-44] that, for spin-1 particles, the plus component of the electromagnetic current, (“ $J^+$ ”), is not free from the pair term contributions (or non-valence contributions) within the Breit frame ( $q^+ = 0$ ), and, thus, that the rotational symmetry is broken.

In general, the matrix elements of the electromagnetic current in the light-front formalism have other contributions besides the valence contribution, namely the pair terms [23, 32, 39, 43], in which the covariance is restored. If the pair term contribution is taken correctly, it does not matter which component of the electromagnetic current is used to extract the electromagnetic form factors of the hadrons. In the present work, two types of the vertex functions for the  $\pi - q\bar{q}$  vertex are assumed to calculate the pion electromagnetic form-factor, and results for the both cases are compared with experimental data [45–51]. In the lower momentum transfer region, non-perturbative regime of QCD is more important than the perturbative regime, the latter working better in the higher momentum transfer region.

Studies of light-vector and pseudoscalar mesons in the light-front approach are very important, since they can pro-

vide a hint of the non-perturbative regime of QCD, and those involving the light-pseudoscalar mesons can shed light on the (spontaneous) chiral symmetry breaking. Properties of such mesons are also studied with other approaches [14,19,37,38,52-67], as well as with the lattice formulation in the light-front [68].

For the lightest pseudoscalar meson, pion, the models based on the Schwinger-Dyson approach [52, 54] describe the electromagnetic form factor quite well. However, some differences amongst the models including the light-front approach can be noticed. Here, we take the light-front models for the pion, presented in previous works [13,23], and extend it to study the higher momentum transfer region and compare with other approaches such as the vector meson dominance [69, 70].

This paper is organized as follows. In Sec. 2, the model of the wave function for the pion, the quark-antiquark bound state in the light-front, is presented, and the electromagnetic form factor is calculated for both non-symmetric and symmetric  $\pi - q\bar{q}$  vertices. In particular, for the non-symmetric vertex, the plus and minus components of the electromagnetic current are used, and the corresponding two results are shown, including the weak decay constant of the pion. In Sec. 3, the vector dominance model is introduced and compared with the light-front approach used. In Sec. 4, numerical results and discussions are presented and, finally, the conclusions are given in Sec. 5.

## 2. Light-front wave function and electromagnetic current

One of the main goals in the light-front approach is to solve the bound state equation,

$$H_{LF}|\Psi\rangle = M^2|\Psi\rangle, \quad (1)$$

where  $H_{LF}$  is the light-front Hamiltonian and  $M^2$  is the invariant mass associated with the physical particle, the eigenstate of the the light-front Hamiltonian [2]. The light-front wave function relates to the Bethe-Salpeter wave function (see [23] for more details). With the light-front wave function it is possible to calculate the matrix elements of the bound states. The meson state may be expressed by a superposition of all Fock states:

$$|\Psi_{meson}\rangle = \Psi_{q\bar{q}}|q\bar{q}\rangle + \Psi_{q\bar{q}g}|q\bar{q}g\rangle + \dots \quad (2)$$

The electromagnetic current where  $J^\mu$ , is expressed in terms of the quark fields and the charge, *i.e.*,  $J^\mu = \sum_f e_f \bar{q}_f \gamma_\mu q_f$ , with  $e_f$  and  $q_f$  being, respectively, the charge and quark field of the flavor  $f$  quark. In this way, the matrix elements of the electromagnetic current are given by

$$\begin{aligned} J^\mu &= -i2e \frac{m^2}{f_\pi^2} N_c \int \frac{d^4k}{(2\pi)^4} \\ &\times Tr \left[ S(k) \gamma^5 S(k-p') \gamma^\mu S(k-p) \gamma^5 \right] \\ &\times \Gamma(k, p') \Gamma(k, p), \end{aligned} \quad (3)$$

where  $S(p) = 1/\not{p} - m + i\epsilon$  is the quark propagator,  $N_c = 3$  is the number of colors and  $m$  is the constituent quark mass. The factor 2 appears from the isospin algebra [13, 23].

The pion quark-antiquark vertex is constrained by the pseudoscalar attributes for the pion [29, 65, 66, 71]. In the present work, we use the similar approach developed some years ago by Frederico and Miller [72], where an effective Lagrangian for the pion quark vertex was utilized, considering only the most important component of the vertex function for the Bethe-Salpeter amplitude, *i.e.*, proportional to  $\gamma^5$ . This effective Lagrangian is associated to the meson vertex, in order to build the spin and flavour structure of the pion meson.

The function  $\Gamma(k, p)$  in Eq. (3) is the regulator vertex function to regularize the Feynman amplitude, *i.e.*, the triangle diagram for the electromagnetic current. Here, we use two possible  $\pi - q\bar{q}$  vertex functions. The first one is the non-symmetric vertex, used in the previous work [13, 73],

$$\Gamma^{(NSY)}(k, p) = \left[ \frac{N}{((p-k)^2 - m_R^2 + i\epsilon)} \right], \quad (4)$$

while the second one is a symmetric vertex, used in Refs. [23, 28]:

$$\Gamma^{(SY)}(k, p) = \left[ \frac{N}{(k^2 - m_R^2 + i\epsilon)} + \frac{N}{((p-k)^2 - m_R^2 + i\epsilon)} \right]. \quad (5)$$

In equation the above,  $m_R$  is the regulator mass used to keep the amplitudes finite, and represents the soft effects at the short range. An important property in the electromagnetic processes is the current conservation, or the gauge invariance. The calculation is performed within the Breit frame; the initial and final momenta of the bound system are, respectively,  $p^\mu = (p_0/2, -q/2 \cos \alpha, 0, -q/2 \sin \alpha)$  and  $p'^\mu = (p_0/2, q/2 \cos \alpha, 0, q/2 \sin \alpha)$ . The transferred momentum is  $q^\mu = (0, q \cos \alpha, 0, q \sin \alpha)$  and the spectator quark momentum is  $k^\mu$ .

The current conservation must be satisfied with the inclusion of the two vertex functions,  $\Gamma(k, p)$ , as used in the present work. This conservation is indeed easily proved within Breit frame (see Ref. [39] for the proof).

The plus component of the electromagnetic current,  $J^+$ , is used to extract the pion electromagnetic form factor, where the Dirac “plus” matrix is given by  $\gamma^+ = \gamma^0 + \gamma^3$ . The plus component ( $J_\pi^+ = J^0 + J^3$ ) of the electromagnetic current for the pion, calculated in the light-front formalism through the triangle Feynman diagram in the impulse approximation, which represents the photon absorption process by the hadronic bound state of the  $q\bar{q}$  pair, is given by:

$$\begin{aligned}
 J_\pi^+ &= e(p^+ + p'^+) F_\pi(q^2) = ie \frac{m^2}{f_\pi^2} N_c \int \frac{dk^- dk^+ d^2 k_\perp}{2(2\pi)^4} \frac{Tr[\mathcal{O}^+] \Gamma(k, p') \Gamma(k, p)}{k^+ (k^- - \frac{f_1 - i\epsilon}{k^+})} \\
 &\times \left[ \frac{1}{(p^+ - k^+) (p^- - k^- - \frac{f_2 - i\epsilon}{p^+ - k^+})} \right] \left[ \frac{1}{(p'^+ - k^+) (p'^- - k^- - \frac{f_3 - i\epsilon}{p'^+ - k^+})} \right], \quad (6)
 \end{aligned}$$

where  $f_i$  ( $i = 1, 2, 3$ ) functions above are defined by  $f_1 = k_\perp^2 + m^2$ ,  $f_2 = (p - k)_\perp^2 + m^2$  and  $f_3 = (p' - k)_\perp^2 + m^2$ , and the light-front coordinates by  $a^\pm = a^0 \pm a^3$  and  $\vec{a}_\perp = (a_x, a_y)$  [2, 4].

In the electromagnetic current expression, Eq. (6), the Jacobian for the light-front coordinates transformation is 1/2, and the Dirac trace, for the operator  $\mathcal{O}^+$ , is written (in light-front coordinates) within the Breit frame with Drell-Yan condition ( $q^+ = 0$ ) as where  $f_i$  ( $i = 1, 2, 3$ ) functions above, are defined by,  $f_1 = k_\perp^2 + m^2$ ,  $f_2 = (p - k)_\perp^2 + m^2$  and  $f_3 = (p' - k)_\perp^2 + m^2$ , with the light-front coordinates defined,  $a^\pm = a^0 \pm a^3$  and  $\vec{a}_\perp = (a_x, a_y)$  [13, 73].

In the expression of the electromagnetic current, Eq. (6), the Jacobian for the transformation to the light-front coordinates is 1/2, and the Dirac trace in the Eq. (6) for the operator  $\mathcal{O}^+$  is written in the light-front coordinates as, in the Breit frame with Drell-Yan condition ( $q^+ = 0$ ), as,

$$Tr[\mathcal{O}^+] = \left[ -4k^- (P'^+ - k^+) (P^+ - k^+) + 4(k_\perp^2 + m^2) (k^+ - P^+ - P'^+) - 2\vec{k}_\perp \cdot (\vec{P}'_\perp - \vec{P}_\perp) (P'^+ - P^+) + k^+ q_\perp^2 \right].$$

In this case (Breit frame and Drell-Yan condition, with  $\alpha = 0$ ), we have the following result:

$$Tr[\mathcal{O}^+] = [-4k^- (k^+ - p^+)^2 + 4(k_\perp^2 + m^2)(k^+ - 2p^+) + k^+ q^2].$$

The quadri-momentum integration of Eq. (6) has two contribution intervals: (i)  $0 < k^+ < p^+$  and (ii)  $p^+ < k^+ < p'^+$ , where  $p'^+ = p^+ + \delta^+$ . The first interval, (i), is the contribution to the valence wave function for the electromagnetic form factor and, the second, (ii), corresponds to the pair terms contribution to the matrix elements of the electromagnetic current. In the case of non-symmetric vertex with the plus component of the electromagnetic current, the second interval does not give any contribution to the current matrix elements, because the non-valence terms' contribution is zero [13, 73]. This is not the case for the minus component of the electromagnetic current for the pion, where beyond the valence contribution we have a non-valence contribution [13] for the matrix elements. For the first interval integration, the pole contribution is  $\bar{k}^- = (f_1 - i\epsilon)/k^+$ . After integrating for the light-front energy,  $k^-$ , the electromagnetic form factors with non-symmetric vertex and the plus component of the electromagnetic current are

$$\begin{aligned}
 F_\pi^{+(i)(NSY)}(q^2) &= ie \frac{m^2 N^2}{2p^+ f_\pi^2} N_c \int \frac{d^2 k_\perp dk^+}{(2\pi)^3} \left[ \frac{Tr[\mathcal{O}^+]}{k^+ (p^+ - k^+)^2 (p^+ - k^+)^2} \right. \\
 &\times \left. \frac{\theta(k^+) \theta(P^+ - k^+)}{(p^- - \bar{k}^- - \frac{f_2 - i\epsilon}{p^+ - k^+}) (p^- - \bar{k}^- - \frac{f_3 - i\epsilon}{p^+ - k^+})} \frac{1}{(p^- - \bar{k}^- - \frac{f_4 - i\epsilon}{p^+ - k^+}) (P'^- - \bar{k}^- - \frac{f_5 - i\epsilon}{p^+ - k^+})} \right], \quad (7)
 \end{aligned}$$

The functions  $f_1, f_2$  and  $f_3$  were already defined; the new functions above are  $f_4 = (p - k)_\perp^2 + m_R^2$  and  $f_5 = (p' - k)_\perp^2 + m_R^2$ . The light-front wave function for the pion with the non-symmetric vertex is

$$\Psi^{(NSY)}(x, k_\perp) = \left[ \frac{N}{(1-x)^2 (m_\pi^2 - \mathcal{M}_0^2) (m_\pi^2 - \mathcal{M}_R^2)} \right], \quad (8)$$

where the fraction of the carried momentum by the quark is  $x = k^+/p^+$  and  $\mathcal{M}_R$  function is written as

$$\mathcal{M}_R^2 = \mathcal{M}^2(m^2, m_R^2) = \frac{k_\perp^2 + m^2}{x} + \frac{(p - k)_\perp^2 + m_R^2}{(1-x)} - p_\perp^2. \quad (9)$$

In the pion wave function expression,  $\mathcal{M}_0^2 = \mathcal{M}^2(m^2, m^2)$  is the free mass operator and the normalization constant  $N$  is determined by the condition  $F_\pi(0) = 1$ .

Finally, the pion electromagnetic form factor expressed with the light-front wave function for the non-symmetric vertex function may be written as

$$\begin{aligned}
 F_\pi^{+(i)(NSY)}(q^2) &= \frac{m^2}{p^+ f_\pi^2} N_c \int \frac{d^2 k_\perp dx}{2(2\pi)^3 x} \left[ -4 \left( \frac{f_1}{xp^+} \right) (xp^+ - p^+)^2 + 4f_1 (xp^+ - 2p^+) + xp^+ q^2 \right] \\
 &\times \Psi_f^{*(NSY)}(x, k_\perp) \Psi_i^{(NSY)}(x, k_\perp) \theta(x) \theta(1-x). \quad (10)
 \end{aligned}$$

In the light-front approach, besides the valence contribution for the electromagnetic current, there is also a contribution from the non-valence components [13, 39, 74]. The non-valence components contribution is calculated in the second interval of the integration (ii), through the "dislocation pole method", whose development is in Ref. [39]. The non-valence contribution to the electromagnetic form factor, in this case, is given by

$$\begin{aligned}
F_{\pi}^{+(ii)(NSY)}(q^2) &= \lim_{\delta^+ \rightarrow 0} 2\imath e \frac{m^2 N^2}{2p^+ f_{\pi}^2} N_c \int \frac{d^2 k_{\perp} dk^+}{2(2\pi)^4} \theta(p^+ - k^+) \theta(p'^+ - k^+) \\
&\times \left[ \frac{\text{Tr}[\mathcal{O}^+]}{k^+(p^+ - k^+)^2 (p^+ - k^+)^2} \frac{1}{(p^- - \bar{k}^- - \frac{f_2 - \imath\epsilon}{p^+ - k^+})(p^- - \bar{k}^- - \frac{f_3 - \imath\epsilon}{p^+ - k^+})} \right. \\
&\times \left. \frac{1}{(p^- - \bar{k}^- - \frac{f_4 - \imath\epsilon}{p^+ - k^+})(p'^- - \bar{k}^- - \frac{f_5 - \imath\epsilon}{p'^+ - k^+})} \right] \propto \delta^+ = 0. \tag{11}
\end{aligned}$$

As can be seen in equation Eq. (11), the electromagnetic form factor in the second integration interval is directly proportional to  $\delta^+$ , which tends to zero. Thus, in the case of non-symmetric vertex for the plus component of the electromagnetic current, calculated for Breit frame and the Drell-Yan condition ( $q^+ = 0$ ), the non-valence (or the pair terms) contributions for the pion electromagnetic form factor is zero [13].

For the minus component of the electromagnetic current,  $J_{\pi}^{-}$  ( $= J^0 - J^3$ ), it is possible to extract the pion electromagnetic form factor with the non-symmetric vertex (Eq. (4)). In this case, we have two contributions: the valence, for the wave function, and the non-valence, to the electromagnetic matrix elements of the electromagnetic current [13, 23, 39]. The pion electromagnetic form factor for the minus component of the electromagnetic current,  $J_{\pi}^{-}$ , is related to the Dirac matrix by  $\gamma^{-} = \gamma^0 - \gamma^3$ , as known from the light-front approach [2, 4]. With the non-symmetric vertex, the minus component of the electromagnetic current is given by

$$\begin{aligned}
J_{\pi}^{-(NSY)} &= e(p + p')^{-} F_{\pi}^{-(NSY)}(q^2) = \imath e^2 \frac{m^2}{f_{\pi}^2} N_c \int \frac{d^4 k}{(2\pi)^4} \text{Tr} \left[ \frac{\not{k} + m}{k^2 - m^2 + \imath\epsilon} \right. \\
&\times \left. \gamma^5 \frac{\not{k} - \not{p}' + m}{(p' - k)^2 - m^2 + \imath\epsilon} \gamma^{-} \frac{\not{k} - \not{p} + m}{(p - k)^2 - m^2 + \imath\epsilon} \gamma^5 \Gamma(k, p') \Gamma(k, p) \right]. \tag{12}
\end{aligned}$$

The Dirac trace in Eq. (12), calculated with the light-front approach, results in the following expression:

$$\text{Tr}[\mathcal{O}^{-}] = [-4k^{-2}k^+ - 4p^+(2k_{\perp}^2 + k^+p^+ + 2m^2) + k^-(4k_{\perp}^2 + 8k^+p^+ + q^+ + 4m^2)]. \tag{13}$$

The expression above has terms proportional to  $k^{-2}$  and  $k^-$ . We show below that these terms do not disappear in the second interval integration and contribute to the matrix elements of the minus component of the electromagnetic current.

In order to calculate the pair terms contribution for the minus component of the electromagnetic current in the second interval integration, ( $p^+ < k^+ < p'^+$ ), the  $k^-$  dependence in the trace and the matrix element of the pair terms are written as

$$\begin{aligned}
J_{\pi}^{-(ii)(NSY)} &= \lim_{\delta^+ \rightarrow 0} 2\imath e \frac{m^2}{f_{\pi}^2} N_c \int \frac{d^2 k_{\perp} dk^+}{2(2\pi)^4} \theta(p^+ - k^+) \theta(p'^+ - k^+) \\
&\times \left[ \frac{\text{Tr}[\bar{\mathcal{O}}^{-}]}{k^+(p^+ - k^+)(p'^+ - k^+)} \frac{1}{(k^- - \frac{f_1 - \imath\epsilon}{k^+})(p^- - \bar{k}^- - \frac{f_2 - \imath\epsilon}{p^+ - k^+})} \right. \\
&\times \left. \frac{1}{(p^- - \bar{k}^- - \frac{f_4 - \imath\epsilon}{p^+ - k^+})(p'^- - \bar{k}^- - \frac{f_5 - \imath\epsilon}{p'^+ - k^+})} \right], \tag{14}
\end{aligned}$$

where  $p'^+ = p^+ + \delta^+$  and  $\bar{k}^- = p^- - (f_3 - \imath\epsilon)/(p'^+ - k^+)$ . The pair terms contribution for the minus component of the electromagnetic current is obtained with Eq. (14), and the Breit frame is recovered in the limit  $\delta^+ \rightarrow 0$ ,

$$J_{\pi}^{-(ii)(NSY)} = 4\pi \left( \frac{m_{\pi}^2 + q^2/4}{p^+} \right) \int \frac{d^2 k_{\perp}}{2(2\pi)^3} \sum_{i=2}^5 \frac{\ln(f_i)}{\prod_{j=2, i \neq j}^5 (-f_i + f_j)}. \tag{15}$$

This last equation, Eq. (15), for the minus component of the current with the second interval integration, is not zero and contribute to the electromagnetic current. This contribution is the non-valence terms contribution to the matrix elements of the electromagnetic current.

The pion electromagnetic form factor with the non-valence contribution, built with the minus component of the matrix elements of the electromagnetic current calculated in Eq. (15), has the final structure

$$F_{\pi}^{-(ii)(NSY)}(q^2) = \frac{N^2}{2p^-} \frac{m^2}{f_{\pi}^2} N_c \left( 4\pi \frac{m_{\pi}^2 + q^2/4}{p^+} \right) \int \frac{d^2 k_{\perp}}{2(2\pi)^3} \sum_{i=2}^5 \frac{\ln(f_i)}{\prod_{j=2, i \neq j}^5 (-f_i + f_j)}. \quad (16)$$

The full electromagnetic form factor of the pion, for the minus component of the electromagnetic current, is then the sum of the partial form factors  $F_{\pi}^{-(i)}$  and  $F_{\pi}^{-(ii)}$ ,

$$F_{\pi}^{-(NSY)}(q^2) = \left[ F_{\pi}^{-(i)(NSY)}(q^2) + F_{\pi}^{-(ii)(NSY)}(q^2) \right]. \quad (17)$$

If the pair terms are not taken into account, the rotational symmetry is broken and the covariance is lost for the  $J_{\pi}^{-}$  component of the electromagnetic current, as can be seen in Fig. 1. After we add the pair terms or zero modes contribution to the calculation of the electromagnetic form factor with the minus component of the electromagnetic current, the identity

$$F_{\pi}^{-(NSY)}(q^2) = F_{\pi}^{+(NSY)}(q^2), \quad (18)$$

is obtained and the full covariance is restored.

In the following step, it is employed the symmetric vertex  $\pi - q\bar{q}$  with the plus component, “+”, of the electromagnetic current (Eq. (5)), as applied in Ref. [23]. This vertex is symmetric by the exchange of the quadri-momentum of the quark and the anti-quark. In the light-front coordinates it is written as

$$\Gamma(k, p) = \mathcal{N} \left[ k^+ \left( k^- - \frac{k_{\perp}^2 + m_R^2 - i\epsilon}{k^+} \right) \right]^{-1} + \mathcal{N} \left[ (p^+ - k^+) \left( p^- - k^- - \frac{(p-k)_{\perp}^2 + m_R^2 - i\epsilon}{p^+ - k^+} \right) \right]^{-1}. \quad (19)$$

With the symmetric vertex, the pion valence wave function results in the expression

$$\Psi^{(SY)}(x, \vec{k}_{\perp}) = \left[ \frac{\mathcal{N}}{(1-x)(m_{\pi}^2 - \mathcal{M}^2(m^2, m_R^2))} + \frac{\mathcal{N}}{x(m_{\pi}^2 - \mathcal{M}^2(m_R^2, m^2))} \right] \frac{p^+}{m_{\pi}^2 - M_0^2}. \quad (20)$$

The electromagnetic form factor for the pion valence wave function (above equation) is calculated within the Breit frame, *i.e.*, ( $q^+ = 0$ ),

$$F_{\pi}^{(SY)}(q^2) = \frac{m^2 N_c}{p^+ f_{\pi}^2} \int \frac{d^2 k_{\perp}}{2(2\pi)^3} \int_0^1 dx \left[ k_{on}^- p^{+2} + \frac{1}{4} x p^+ q^2 \right] \times \frac{\Psi_f^{*(SY)}(x, k_{\perp}) \Psi_i^{(SY)}(x, k_{\perp})}{x(1-x)^2},$$

where the on-shell condition for the spectator quark is  $k_{on}^- = (k_{\perp}^2 + m^2)/k^+$  and the normalization constant  $\mathcal{N}$  is determined from the condition  $F_{\pi}^{(SY)}(0) = 1$ . The pion electromagnetic form factor calculated with the symmetric wave function is presented in Fig. 5 for higher momentum and for low momentum transfer. In both regions, the differences between the symmetric and non-symmetric vertex are not very large.

The pion decay constant, measured in the weak leptonic decay, with partial axial current conservation given by  $P_{\mu} < 0 | \bar{q} \gamma^{\mu} \gamma^5 \tau_i q / 2 | \pi_j > = v m_{\pi}^2 \delta_{ij}$  [13, 23] and vertex function  $\Gamma(k, p)$ , is expressed by

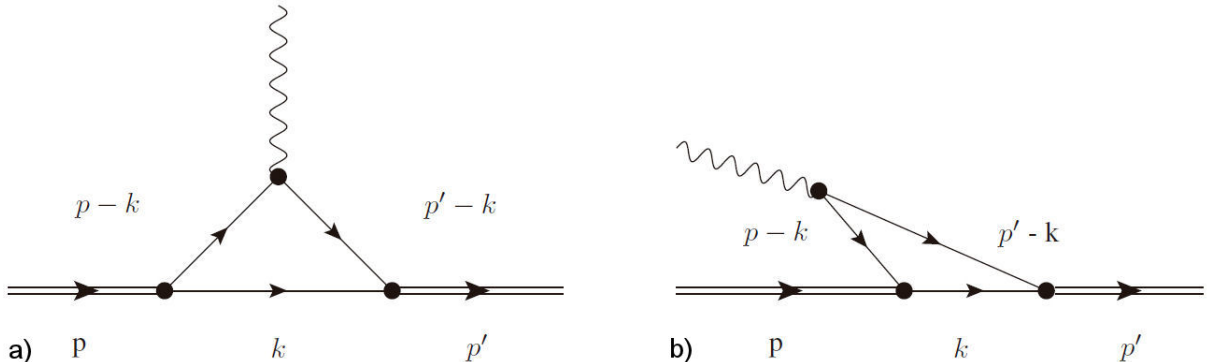


FIGURE 1. Feynman diagrams for the valence contribution a) and the non-valence contribution b) for the electromagnetic current.

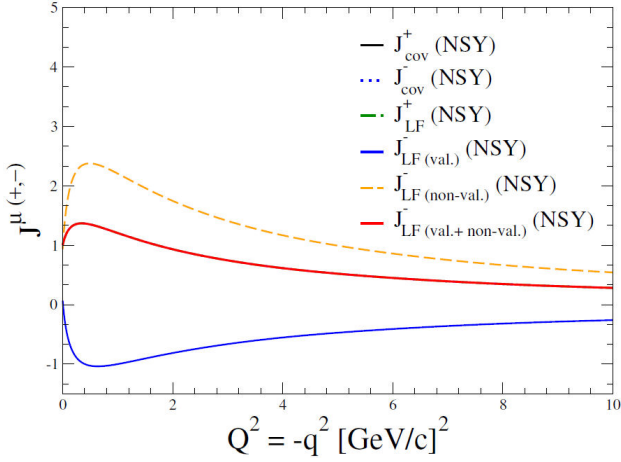


FIGURE 2. The electromagnetic current for the non-symmetric vertex. The range for the momentum transfer given here is up to  $10 \text{ (GeV/c)}^2$

$$if_\pi P^2 = N_c \frac{m}{f_\pi} \int \frac{d^4 k}{(2\pi)^4} \times Tr [\not{p} \gamma^5 S(k) \gamma^5 S(k-p)] \Gamma(k, p). \quad (21)$$

In the case of the non-symmetric and symmetric vertices, (see Eqs. (4) and (5)), the expressions for the decay constant are, respectively,

$$f_{(\pi)}^{(NSY)} = \frac{m^2 N_c}{f_\pi} \int \frac{d^2 k_\perp dx}{4\pi^3 x} \Psi_\pi^{(NSY)}(k^+, \vec{k}_\perp; m, \vec{0}),$$

and,

$$f_{(\pi)}^{(SY)} = \frac{m^2 N_c}{f_\pi} \int \frac{d^2 k_\perp dx}{4\pi^3 x(1-x)} \Psi_\pi^{(SY)}(x, \vec{k}_\perp; m, \vec{0}). \quad (22)$$

The obtained values of the decay constant with the expressions above, for both light-front models calculations, do not have significant discrepancies, and agree with the experimental value [75].

In the next section, the vector meson dominance model (VMD) is presented; subsequently, we compare the VMD with the models presented here so far.

### 3. Vector meson dominance

In the 1960's, J. Sakurai [76, 77] proposed the theory of *Vector Meson Dominance* (VMD): a theory of strong interactions with the local gauge invariance, mediated by vector mesons and based on the non-Abelian field theory of Yang-Mills. It is possible to have two Lagrangian formulations of the vector meson dominance. The first was introduced by Kroll, Lee and Zumino [69] and is customarily called VMD-1. The pion electromagnetic form factor calculated with this formulation results in

$$F_\pi^{VMD1}(q^2) = \left[ 1 - \frac{q^2}{q^2 - m_\rho^2} \frac{g_{\rho\pi\pi}}{g_\rho} \right]. \quad (23)$$

The equation above for the electromagnetic form factor satisfies the condition  $F_\pi(0) = 1$ , independently of any assumption about the coupling constants,  $g_{\rho\pi\pi}$  and  $g_\rho$ .

In the second formulation of the vector meson dominance, the Lagrangian has a photon mass term, and the photon propagator has a non-zero mass; this version is usually called VMD-2. With this second formulation of the vector meson dominance, the pion electromagnetic form factor is written as

$$F_\pi^{VMD2}(q^2) = \left[ -\frac{m_\rho^2}{q^2 - m_\rho^2} \frac{g_{\rho\pi\pi}}{g_\rho} \right]. \quad (24)$$

In the equation above, the condition  $F_\pi(0) = 1$  must be satisfied only if the universality limit is taken into account or translate into the following equality:  $g_{\rho\pi\pi} = g_\rho$ . In the universality limit, as advocated by J. Sakurai, the two formulations of the vector meson dominance are equivalent. For the present work, in Eq. (23) and Eq. (24), the rho meson mass input is the experimental value,  $m_\rho = 0.767 \text{ GeV}$  [75], and, from the universality,  $g_{\rho\pi\pi} = g_\rho$ , the results at zero momentum for both equations satisfy  $F_\pi(0) = 1$ .

In the present case here, only the lightest vector resonance rho meson is taken into account in the monopole model of the VMD expressed in Eq. (23) or Eq. (24). The vector meson dominance works quite well in the time-like region below the  $\pi\pi$  threshold. At low energies, for the space-like region, the vector meson dominance model provides a reasonable description for the pion electromagnetic form factor. For more details and results about the vector meson dominance, see [26, 70, 78].

### 4. Results

The pion electromagnetic form factor, presented consistently with previous works, is extended at higher momentum transfer region, for  $Q^2 = -q^2$  up to  $20 \text{ (GeV/c)}^2$  (see the Fig. 6). The models of the  $\pi - q\bar{q}$  vertices, *i.e.*, non-symmetric and symmetric vertices [13,23], are compared with the vector meson dominance (VMD), and are show in Figs. 5 and 6, for low and higher momentum transfer.

Important consequences are the direct results of the idea that hadrons are a composite system. Such consequences are associated with deep inelastic scattering (DIS), at high transferred moments. The applications of perturbative QCD (pQCD), at transferred high moments, is certainly an extremely interesting physics problem. The pQCD was initially developed in the works of Brodsky and Lepage, among others [65,79-82], predicts a limit for  $Q^2 \gg \Lambda_{QCD} \sim 200 \text{ MeV}$ , given by the expression below,

$$Q^2 F_\pi(Q^2)|_{Q^2 \rightarrow \infty} \longrightarrow 16\alpha_s(Q^2) f_\pi^2, \quad (25)$$

with  $\alpha_s(Q^2)$  is expressed by,

$$\alpha_s(Q^2) = \frac{4\pi}{\beta_0 \ln(Q^2/\Lambda_{QCD})}, \quad \text{here, } \beta_0 = 11 - \frac{2}{3}n_f,$$

where,  $n_f$  is the flavors number. The two models used in the present work, at moments transferred above  $50.0 \text{ GeV}^2$ , are very close to the results obtained with the pQCD.

The pion electromagnetic radius is calculated with the derivative of the electromagnetic form factor for the pion,  $\langle r^2 \rangle = -6dF(q^2)/dq^2_{|q^2 \simeq 0}$ , for both vertex models presented here.

In the case of the non-symmetric vertex, the pion radius is used to fix the parameters of the model. The parameters are the quark mass  $m_q = 0.220 \text{ GeV}$  and the regulator mass  $m_R = 1.0 \text{ GeV}$ . The pion mass used as input is the experimental value,  $m_\pi = 0.140 \text{ GeV}$ . The experimental radius of the pion is  $r_{exp} = 0.672 \pm 0.02 \text{ fm}$  [45, 75]. Using the pion decay constant calculation in the non-symmetric vertex model and with the parameters above, the pion decay constant obtained is  $f_\pi = 92.13 \text{ MeV}$ , which is close to the experimental value,  $f_\pi \simeq 92.28(7)$  [75].

On the other hand, for the symmetric vertex, the parameters are the quark mass  $m_q = 0.220 \text{ GeV}$ , the regulator mass  $m_R = 0.600 \text{ GeV}$  and the experimental mass of the pion  $m_\pi = 0.140 \text{ GeV}$ . Our choice for the regulator mass fits the experimental pion decay constant quite well when compared to the experimental data [75]. Also, good results are obtained for the electromagnetic pion radius for both vertex models. Both light-front models, with symmetric and non-symmetric vertices, are in good agreement with the experimental data at low energy; however, some differences are

TABLE I. Results for the low-energy electromagnetic  $\pi$ -meson observables with the light-front models presented here. Immediately below are values from other models in the literature.

Model	$r_\pi$ (fm)	$f_\pi$ (MeV)	$r_\pi \cdot f_\pi$
Non-Sym. Vert.(LF)	0.672	93.13	0.316
Sym.Vert. (LF)	0.736	92.40	0.345
Kissilinger <i>et al.</i> [25]	0.651	91.91	0.304
Silva <i>et al.</i> [73]	0.672	101.0	0.343
Maris & Tandy [83]	0.671	92.62	0.315
Faessler <i>et al.</i> [84]	0.65	92.62	0.304
Ebert <i>et al.</i> [85, 86]	0.66	109.60	0.367
Bashir <i>et al.</i> [87]		101.0	
Chen & Chang [88]		93.0	
Hutauruk <i>et al.</i> [89]	0.629	93.0	0.308
Ivanov <i>et al.</i> [90]		92.14	
Jia & Vary [91]	0.68(5)	142.8	0.491
Maris & Roberts [92]	0.550	92.0	0.256
Chang <i>et al.</i> [65]	0.66	92.2	0.307
Eichmann [93]		92.4(2)	
Miramontes <i>et al.</i> [94]	0.685 ( $\eta = 1.5$ )	97.57	0.339
Miramontes <i>et al.</i> [94]	0.683 ( $\eta = 1.6$ )	97.57	0.338
Dominguez <i>et al.</i> [95]	0.631		
Exp. [75]	0.672(8)	92.28(7)	0.313

noticeable in the  $Q^2 \geq 1.0 \text{ GeV}^2$  region (see Fig. 5). The experimental data collected from [47] worked well up to  $10 \text{ GeV}^2$  for both the symmetric and non-symmetric vertex functions. For the minus component of the electromagnetic current,  $J^-$ , the pair terms or non-valence components of the electromagnetic current contributions are essential to obtain the full covariant pion electromagnetic form factor while respecting the covariance.

In Table II we show the non-valence contribution to the electromagnetic current calculated with the light-front approach for some values of the momentum transfer, for both instant form and light-front approaches. It is worth noting that as there are no contributions due to valence terms or zero modes, results for the covariant calculations with both components of the electromagnetic current, *i.e.*, plus and minus components,  $J^{+(Cov.)}$ ,  $J^{-(Cov.)}$ , are exactly the same.

One can also see the need to add zero modes to the electromagnetic current matrix elements for the minus component of the electromagnetic current case. The constituents quark models formulated with the light-front approach presented here are in good agreement with experimental data [45-48,50,51].

The results presented in Table II can be visualized in Fig. 2, where we show, for both components of the electromagnetic current, the calculations with both formalism: the covariant and the light-front approaches.

The plus component,  $J^+$ , of the electromagnetic current for the symmetric vertex case, considered in this work, is presented in the left panel of Fig. 3, for the case where the angle  $\alpha$  is equal to zero (and within the Breit frame with the Drell-Yan condition). It can be seen that, the non-valence contributions do not contribute to the matrix elements of the electromagnetic current in this case.

The ratios between the electromagnetic current in the light-front and the electromagnetic current, calculated in the instant form, are given by the following equations:

TABLE II. Numerical results for the plus and minus components of the electromagnetic currents ( $J^+$ ,  $J^-$ ), with some values for the momentum transfer, for both cases of the models considered here: non-symmetric vertex model from [13], calculated with the covariant and with the light-front approaches. Labels are: (I- $J^{+(Cov.)}$ ), (II- $J^{-(Cov.)}$ ), (III- $J^{+(NSYV)}$ ), (IV- $J^{-(NSYV)}$ ), (V- $J^{-(NVAL:(NSY))}$ ), and (VI- $J^{-(VAL+NVAL)}$ ). The momentum  $Q^2$  is given in [ $\text{GeV}^2$ ].

$Q^2$	I	II	III	IV	V	VI
2.0	0.932	0.932	0.932	-0.814	1.746	0.932
4.0	0.613	0.613	0.613	-0.553	1.167	0.613
6.0	0.448	0.448	0.448	-0.409	0.858	0.448
8.0	0.346	0.346	0.346	-0.317	0.666	0.346
10.0	0.281	0.281	0.282	-0.260	0.541	0.281

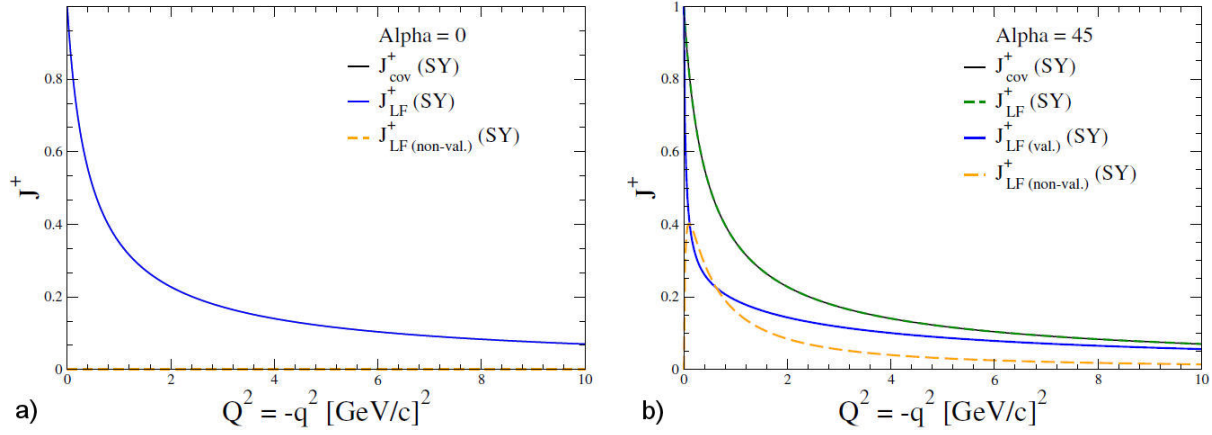


FIGURE 3. The electromagnetic current for the symmetric vertex, with referential angle 0.0 a) and 45 degrees b). The range for the momentum transfer given here is up to 10 (GeV/c)<sup>2</sup>.

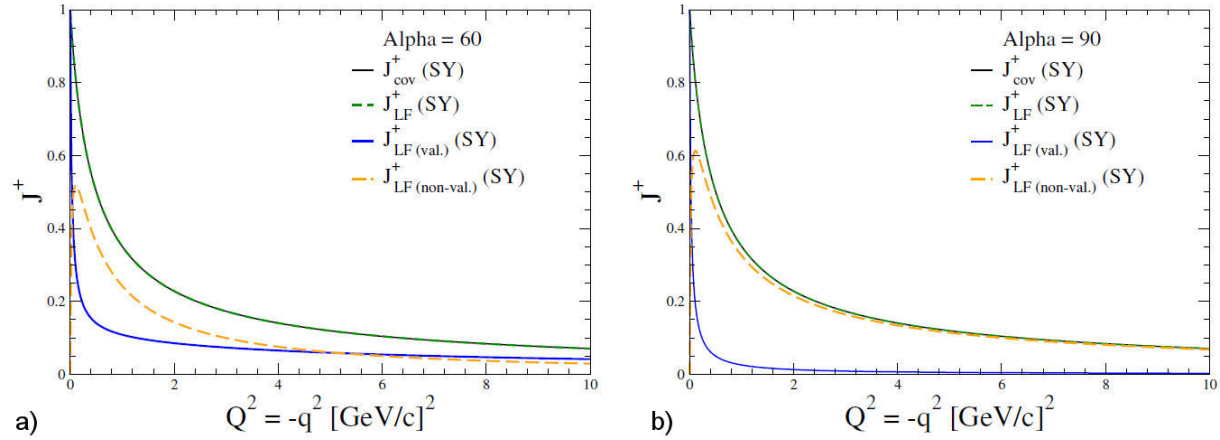


FIGURE 4. The electromagnetic current for the symmetric vertex, with referential angle 60 a) and 90 degrees b). The range for the momentum transfer given here is up to 10 (GeV/c)<sup>2</sup>.

$$\begin{aligned}
 Ra^I &= \frac{J_{LF}^{+(NSYV)}}{J_{Cov}^{+(NSYV)}}, \\
 Ra^{II} &= \frac{J_{LF}^{-(NSYV(val.))}}{J_{Cov}^{-(NSYV)}}, \\
 Ra^{III} &= \frac{J_{LF}^{-(NSYV(val.))} + J_{LF}^{-(NSYV(nval.))}}{J_{Cov}^{-(NSYV)}}, \\
 Ra^{IV} &= \frac{J_{LF}^{+(SYV(val.+nval.))}}{J_{Cov}^+} \Big|_{(\alpha=0)}, \\
 Ra^V &= \frac{J_{LF}^{+(SYV(val.))}}{J_{Cov}^+} \Big|_{\alpha=90}, \\
 Ra^{VI} &= \frac{J_{LF}^{+(SYV(val.+nval.))}}{J_{Cov}^+} \Big|_{(\alpha=90)}, \quad (26)
 \end{aligned}$$

where the non-symmetric vertex, and symmetric vertex, are utilized according to Eqs. (4) and Eq. (5), respectively.

In Eq. (26), the ratio  $Ra^I$  is the plus component of the electromagnetic current calculated in the light-front approach divided by the electromagnetic current calculated in the instant form; both calculated with the non-symmetric vertex model [23]. Since the pair terms do not contribute for the plus component of the electromagnetic current, the ratio  $Ra^I$  is constant (see Fig. 7).

The second ratio,  $Ra^{II}$ , is the minus component of the electromagnetic current,  $J^-$ , calculated with the light-front formalism and divided by the electromagnetic current calculated in the instant form. In  $Ra^{III}$  ratio, the pair terms contribution to the electromagnetic current is included, so the covariance is restored.

The ratios  $Ra^{IV}$  and  $Ra^V$  are the “minus” components of the electromagnetic current without and with the pair terms contribution, respectively, divided by the “plus” component of the electromagnetic current calculated in the instant form.

As can be seen in Fig. 2, the rotational symmetry in the light-front formalism is broken; this happens because the pair terms or non-valence contribution for the electromagnetic



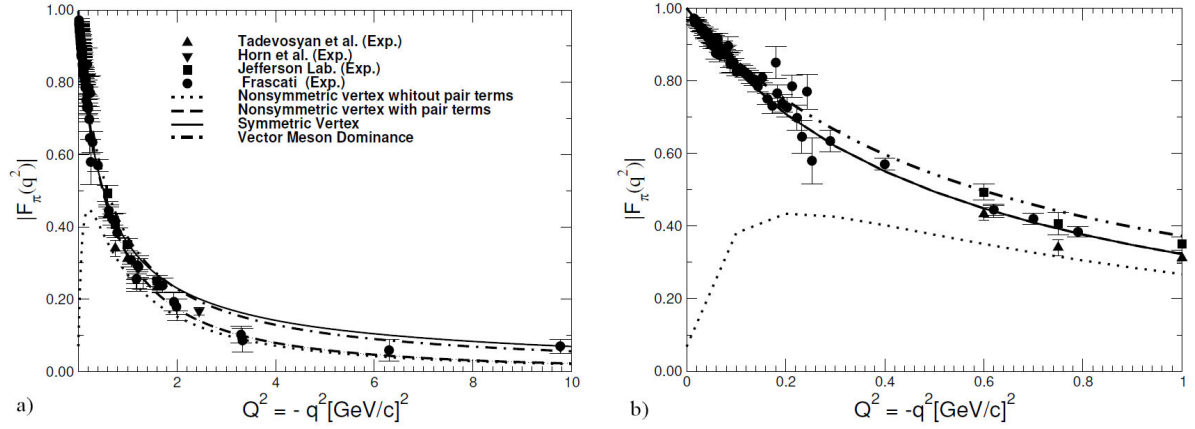


FIGURE 5. a) Pion electromagnetic form factor calculated with light-front constituent quark model, for the plus and minus components of electromagnetic current, compared with experimental data and vector meson dominance. Data are from [47, 48, 50, 51]. Solid line is the full covariant form factor with  $J_\pi^+$  (symmetric vertex for the  $\pi - q\bar{q}$ ). The dashed line is line the form factor with  $J_\pi^-$  plus pair terms contribution, and the dotted line is the pion form factor without the pair terms contribution with the minus component of the electromagnetic current, where both curves are with the nonsymmetric vertex. After added the non-valence contribution, the pion electromagnetic form factor calculated with the plus or minus component of the electromagnetic current give the same results for the nonsymmetric vertex. b) Pion electromagnetic form factor for small  $Q^2$ . Labels are the same as the left panel.

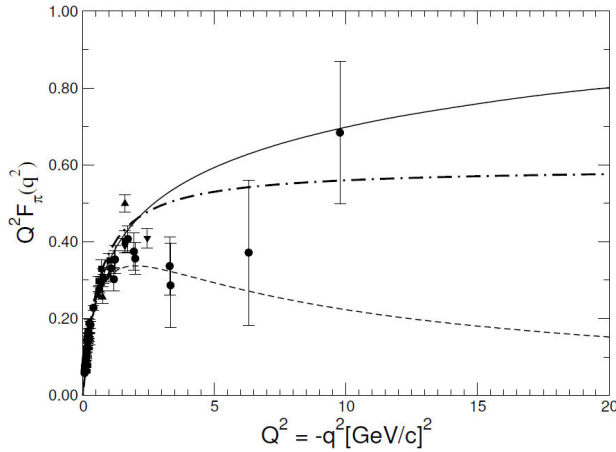


FIGURE 6. Pion electromagnetic form factor for higher  $Q^2$ . Labels are the same as those in Fig. 5.

current is not taken into account properly. The restoration of the symmetry breaking is obtained by adding the pair terms contribution to the minus component of the electromagnetic current calculated in the light-front.

Experimental data for  $Q^2 \gtrsim 1.5 \text{ GeV}/c^2$  for the pion electromagnetic form factor (see Fig. 5) are not precise enough in order to satisfactorily select, amongst the phenomenological models, which is the best description for the pion elastic electromagnetic form factor or, in other words, the correct pion wave function.

Results displayed in Fig. 6 confirm the validity of the vector meson dominance model at very low momentum transfer ( $Q^2 \leq 0.5 \text{ GeV}/c^2$ ).

For  $Q^2 > 0.5 \text{ GeV}/c^2$  (see Fig. 5), however, the discrepancies between the vector meson dominance model, the light-front models and experimental data are more prominent.

In the case of  $\Delta_3$ , (see definition above), the covariance is respected because the difference is zero in the integration sum interval, [(i)+(ii)], for the  $J^-$  component of the electromagnetic current. The electromagnetic form factor for the pion calculated with the matrix elements of the electromagnetic current provides the same results as the electromagnetic form factor of the pion calculated with usual covariant quantum field theory [5].

In order to compare the breaking magnitude of the rotational symmetry for the pion electromagnetic form factor with light-front models, the vector meson dominance model, and the one with covariant calculations, we define the following equations in an attempt to amplify the differences amongst these theoretical models and experimental data:

$$\begin{aligned}
 \Delta_1 &= \left[ q^2 F_\pi^{COV(NSYV)}(q^2) - q^2 F_\pi^{+(NSYV)}(q^2) \right], \\
 \Delta_2 &= \left[ q^2 F_\pi^{(COV(NSYV))}(q^2) - q^2 F_\pi^{-(val.)(NSYV)}(q^2) \right], \\
 \Delta_3 &= \left[ q^2 F_\pi^{(COV(NSYV))}(q^2) \right. \\
 &\quad \left. - q^2 F_\pi^{-(val.+nonval.)(NSYV)}(q^2) \right], \\
 \Delta_4 &= \left[ q^2 F_\pi^{(COV(SYV))}(q^2) - q^2 F_\pi^{(val.)(SYV)}(q^2) \right], \\
 &\quad (\alpha = 0.0), \\
 \Delta_5 &= \left[ q^2 F_\pi^{(COV(SYV))}(q^2) - q^2 F_\pi^{SYV}(q^2) \right], \\
 &\quad (\alpha = 60), \\
 \Delta_6 &= \left[ q^2 F_\pi^{(COV(SYV))}(q^2) - q^2 F_\pi^{SYV}(q^2) \right], \\
 &\quad (\alpha = 90). \tag{27}
 \end{aligned}$$

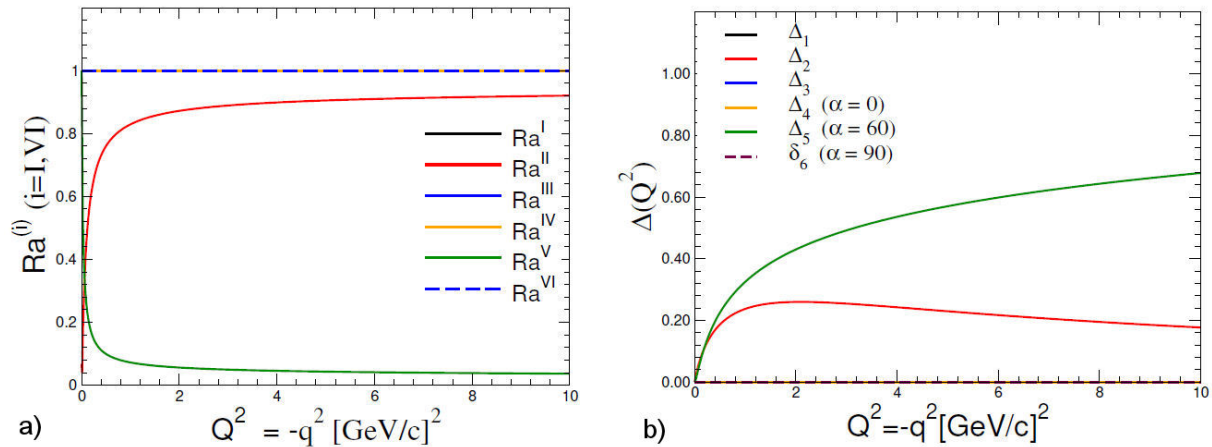


FIGURE 7. a) Ratios for the pion electromagnetic current (see Eq. (26) in the text). b) Labels are the same as those in Eq. (27). The range for the momentum transfer given here is up to  $10 (\text{GeV}/c)^2$ .

The results of the calculations with the Eq. (27), are shown in the Fig. (7) (right panel), up to  $10 \text{ GeV}^2$ .

For the higher momentum transfer, the asymptotic behavior for the wave function of the non-symmetric vertex model produce  $q^2 F_\pi(15 \text{ GeV}^2/c^2) \approx 0.18 (\text{GeV}/c)^2$ . That result is compared with the leading-order-perturbative QCD,  $Q^2 F_\pi(Q^2) \approx 0.15 (\text{GeV}/c)^2$ , for  $\alpha_s(Q^2 = 10 (\text{GeV}/c)^2) \approx 0.3$  and with Dyson-Schwinger approach,  $Q^2 F_\pi(Q^2) \approx 0.12 - 0.19 (\text{GeV}/c)^2$ , for momentum transfer between  $Q^2 \approx 10 - 15 (\text{GeV}/c)^2$  [92].

## 5. Conclusions

In this work, the electromagnetic form factor of the pion was investigated in the range  $0 < Q^2 < 20 \text{ GeV}/c^2$  with the light-front constituent quark model. The light-front formalism is known nowadays as a natural way to describe the systems with relativistic bound state, such as the pion. With this approach it is possible to calculate the electromagnetic form factors in a more suitable way.

However, issues related with the breaking of the rotational symmetry in the light-front formalism become relevant and the pair terms or non-valence terms contribution for the covariance restoration in higher energies need some attention [13, 31].

After adding the non-valence components in the matrix elements of the electromagnetic current, the covariance is completely restored, and it does not matter which component of the electromagnetic current,  $J^+$  or  $J^-$ , is used to extract the pion form factor with the light-front approach, as shown in Fig. 5.

The numerical results presented in Fig. 4 show the importance of the non-valence components for the electromagnetic current and the dependence with the choice of the component used at low momentum transfer. To achieve the full covariance, the inclusion of the non-valence components is essential for the minus component of the electromagnetic current.

In Eq. (26), the ratios  $Ra^I$ ,  $Ra^{III}$  and  $Ra^V$ , produce constant values, but the ratios  $Ra^{II}$  and  $Ra^{IV}$  do not, because the non-valence components of the electromagnetic current is not included in the light-front approach calculation (see Fig. 7).

The light-front models for the vertex  $\pi - q\bar{q}$  and other hadronic models for the pion electromagnetic form-factor show good agreement between them; however, some differences arise when energies are in the higher region,  $Q^2 \gtrsim 2 \text{ GeV}/c^2$ .

From Eq. (27), the differences between the models analyzed in this work are clear, either for lower or higher momentum transfer, because the set of equations intensifies the non-similarities amongst the models.

Since the pion electromagnetic form-factor is sensitive to the model adopted, it is important to compare different models, including new experimental data, and to extract new information about the sub-hadronic structure of the pion bound state.

The light-front approach is a good framework to study the pion electromagnetic form factor. Nonetheless, the inclusion of the non-valence components of the electromagnetic current is essential for both low and higher momentum transfer.

We conclude that the light-front formalism and the vertex models for  $\pi - q\bar{q}$ , with symmetric and non-symmetric vertices describe the new experimental data for the pion electromagnetic form factor with very good agreement. As a next step, calculations for the vector mesons, like  $\rho$ -meson and vector kaon, are in progress in order to allow us to also compare these with the light-front constituent models.

## Acknowledgments

This work was supported in part by the Conselho Nacional de Desenvolvimento Científico e Tecnológico (CNPq), Grant Process, No. 307131/2020-3 (JPBCM), and Fundação de Amparo à Pesquisa do Estado de São Paulo (FAPESP), Process, No. 2019/02923-5, and was also part of the projects,

Instituto Nacional de Ciência e Tecnologia, Física Nuclear e Aplicações (INCT-FNA), Brazil, Process No. 464898/2014-

5, and FAPESP Temático, Brazil, Process, the thematic projects, No. 2013/26258-4 and No. 2017/05660-0.

1. P. A. M. Dirac, Forms of Relativistic Dynamics, *Rev. Mod. Phys.* **21** (1949) 392, <https://doi.org/10.1103/RevModPhys.21.392>.
2. S. J. Brodsky, H.-C. Pauli, and S. S. Pinsky, Quantum chromodynamics and other field theories on the light cone, *Phys. Rept.* **301** (1998) 299, [https://doi.org/10.1016/S0370-1573\(97\)00089-6](https://doi.org/10.1016/S0370-1573(97)00089-6).
3. M. Lacombe *et al.*, Testing the quark cluster model in nucleon-nucleon scattering, *Phys. Rev. C* **65** (2002) 034004, <https://doi.org/10.1103/PhysRevC.65.034004>.
4. A. Harindranath, Light front quantum chromodynamics: Towards phenomenology, *Pramana* **55** (2000) 241, <https://doi.org/10.1007/s12043-000-0100-7>.
5. C. Itzykson and J.-B. Zuber, Quantum field theory (Courier Corporation, 2012), McGraw-Hill, New York, International Series In Pure and Applied Physics, ISBN 978-0-486-44568-7.
6. R. J. Perry, A. Harindranath, and K. G. Wilson, Light front Tamm-Dancoff field theory, *Phys. Rev. Lett.* **65** (1990) 2959, <https://doi.org/10.1103/PhysRevLett.65.2959>.
7. M. V. Terentev, On the Structure of Wave Functions of Mesons as Bound States of Relativistic Quarks, *Sov. J. Nucl. Phys.* **24** (1976) 106
8. W. R. B. de Araujo, J. P. B. C. de Melo, and T. Frederico, Faddeev null plane model of the nucleon, *Phys. Rev. C* **52** (1995) 2733, <https://doi.org/10.1103/PhysRevC.52.2733>.
9. Z. Dziembowski and L. Mankiewicz, LIGHT MESON DISTRIBUTION AMPLITUDE: A SIMPLE RELATIVISTIC MODEL, *Phys. Rev. Lett.* **58** (1987) 2175, <https://doi.org/10.1103/PhysRevLett.58.2175>.
10. F. Cardarelli *et al.*, Nucleon and pion electromagnetic form-factors in a light front constituent quark model, *Phys. Lett. B* **357** (1995) 267, [https://doi.org/10.1016/0370-2693\(95\)00921-7](https://doi.org/10.1016/0370-2693(95)00921-7).
11. F. Cardarelli *et al.*, Charge form-factor of pi and K mesons, *Phys. Rev. D* **53** (1996) 6682, <https://doi.org/10.1103/PhysRevD.53.6682>.
12. A. F. Krutov and V. E. Troitsky, On a possible estimation of the constituent quark parameters from Jefferson Lab experiments on pion form-factor, *Eur. Phys. J. C* **20** (2001) 71, <https://doi.org/10.1007/s100520100642>.
13. J. P. C. B. de Melo, H. W. L. Naus, and T. Frederico, Pion electromagnetic current in the light cone formalism, *Phys. Rev. C* **59** (1999) 2278, <https://doi.org/10.1103/PhysRevC.59.2278>.
14. A. F. Krutov, V. E. Troitsky, and N. A. Tsirova, Nonperturbative relativistic approach to pion form factor versus JLab experiments, *Phys. Rev. C* **80** (2009) 055210, <https://doi.org/10.1103/PhysRevC.80.055210>.
15. D. Melikhov and S. Simula, Electromagnetic form-factors in the light front formalism and the Feynman triangle diagram: Spin 0 and spin 1 two fermion systems, *Phys. Rev. D* **65** (2002) 094043, <https://doi.org/10.1103/PhysRevD.65.094043>.
16. J. P. B. C. de Melo *et al.*, Electromagnetic form-factor of the pion in the space and time - like regions within the front form dynamics, *Phys. Lett. B* **581** (2004) 75, <https://doi.org/10.1016/j.physletb.2003.11.072>.
17. H.-Y. Cheng, C.-K. Chua, and C.-W. Hwang, Covariant light front approach for s wave and p wave mesons: Its application to decay constants and form-factors, *Phys. Rev. D* **69** (2004) 074025, <https://doi.org/10.1103/PhysRevD.69.074025>.
18. T. Huang and X.-G. Wu, A Model for the twist-3 wave function of the pion and its contribution to the pion form-factor, *Phys. Rev. D* **70** (2004) 093013, <https://doi.org/10.1103/PhysRevD.70.093013>.
19. V. V. Braguta and A. I. Onishchenko, Pion form-factor and QCD sum rules: Case of axial current, *Phys. Lett. B* **591** (2004) 267, <https://doi.org/10.1016/j.physletb.2004.04.029>.
20. L. A. M. Salcedo *et al.*, Weak decay constant of pseudoscalar meson in a QCD inspired model, *Braz. J. Phys.* **34** (2004) 297, <https://doi.org/10.1590/S0103-97332004000200034>.
21. L. A. M. Salcedo *et al.*, Electromagnetic structure and weak decay of pseudoscalar mesons in a light-front QCD-inspired model, *Eur. Phys. J. A* **27** (2006) 213, <https://doi.org/10.1140/epja/i2005-10246-4>.
22. V. A. Karmanov, J. F. Mathiot, and A. V. Smirnov, Regularization of fermion self-energy and electromagnetic vertex in Yukawa model within light-front dynamics, *Phys. Rev. D* **75** (2007) 045012, <https://doi.org/10.1103/PhysRevD.75.045012>.
23. J. P. B. C. de Melo *et al.*, Pair term in the electromagnetic current within the front form dynamics: Spin-0 case, *Nucl. Phys. A* **707** (2002) 399, [https://doi.org/10.1016/S0375-9474\(02\)00990-9](https://doi.org/10.1016/S0375-9474(02)00990-9).
24. B. L. G. Bakker, H.-M. Choi, and C.-R. Ji, Regularizing the fermion loop divergencies in the light front meson currents, *Phys. Rev. D* **63** (2001) 074014, <https://doi.org/10.1103/PhysRevD.63.074014>.
25. L. S. Kisslinger, H.-M. Choi, and C.-R. Ji, Pion form-factor and quark mass evolution in a light front Bethe-Salpeter model, *Phys. Rev. D* **63** (2001) 113005, <https://doi.org/10.1103/PhysRevD.63.113005>.
26. J. P. B. C. de Melo *et al.*, Space-like and time-like pion electromagnetic form-factor and Fock state components within the light-front dynamics, *Phys. Rev. D* **73** (2006) 074013, <https://doi.org/10.1103/PhysRevD.73.074013>.

27. E. P. Biernat *et al.*, Pion electromagnetic form factor in the Covariant Spectator Theory, *Phys. Rev. D* **89** (2014) 016006, <https://doi.org/10.1103/PhysRevD.89.016006>.
28. G. H. S. Yabusaki *et al.*, Pseudoscalar mesons with symmetric bound state vertex functions on the light front, *Phys. Rev. D* **92** (2015) 034017, <https://doi.org/10.1103/PhysRevD.92.034017>.
29. T. Horn and C. D. Roberts, The pion: an enigma within the Standard Model, *J. Phys. G* **43** (2016) 073001, <https://doi.org/10.1088/0954-3899/43/7/073001>.
30. L. Adhikari *et al.*, Form Factors and Generalized Parton Distributions in Basis Light-Front Quantization, *Phys. Rev. C* **93** (2016) 055202, <https://doi.org/10.1103/PhysRevC.93.055202>.
31. J. P. B. C. de Melo and T. Frederico, Covariant and light front approaches to the rho meson electromagnetic form-factors, *Phys. Rev. C* **55** (1997) 2043, <https://doi.org/10.1103/PhysRevC.55.2043>.
32. J. P. B. C. de Melo *et al.*, Covariance of light front models: Pair current, *Nucl. Phys. A* **660** (1999) 219, [https://doi.org/10.1016/S0375-9474\(99\)00371-1](https://doi.org/10.1016/S0375-9474(99)00371-1).
33. F. M. Lev, E. Pace, and G. Salme, Deuteron magnetic and quadrupole moments with a Poincare covariant current operator in the front form dynamics, *Phys. Rev. Lett.* **83** (1999) 5250, <https://doi.org/10.1103/PhysRevLett.83.5250>.
34. F. M. Lev, E. Pace, and G. Salme, Poincare covariant current operator and elastic electron deuteron scattering in the front form Hamiltonian dynamics, *Phys. Rev. C* **62** (2000) 064004, <https://doi.org/10.1103/PhysRevC.62.064004>.
35. W. Jaus, Consistent treatment of spin 1 mesons in the light front quark model, *Phys. Rev. D* **67** (2003) 094010, <https://doi.org/10.1103/PhysRevD.67.094010>.
36. J. P. B. C. de Melo *et al.*, Frame dependence of the pair contribution to the pion electromagnetic form-factor in a light front approach, *Braz. J. Phys.* **33** (2003) 301, <https://doi.org/10.1590/S0103-97332003000200027>.
37. T. M. Aliev and M. Savci, Electromagnetic form factors of the rho meson in light cone QCD sum rules, *Phys. Rev. D* **70** (2004) 094007, <https://doi.org/10.1103/PhysRevD.70.094007>.
38. V. V. Braguta and A. I. Onishchenko, rho meson form-factors and QCD sum rules, *Phys. Rev. D* **70** (2004) 033001, <https://doi.org/10.1103/PhysRevD.70.033001>.
39. H. W. L. Naus, J. P. B. C. de Melo, and T. Frederico, Ward-Takahashi identity on the light front, *Few Body Syst.* **24** (1998) 99, <https://doi.org/10.1007/s006010050080>.
40. B. L. G. Bakker, H.-M. Choi, and C.-R. Ji, Transition form-factors between pseudoscalar and vector mesons in light front dynamics, *Phys. Rev. D* **67** (2003) 113007, <https://doi.org/10.1103/PhysRevD.67.113007>.
41. H.-M. Choi and C.-R. Ji, Electromagnetic structure of the rho meson in the light front quark model, *Phys. Rev. D* **70** (2004) 053015, <https://doi.org/10.1103/PhysRevD.70.053015>.
42. B. L. G. Bakker, H.-M. Choi, and C.-R. Ji, The Vector meson form-factor analysis in light front dynamics, *Phys. Rev. D* **65** (2002) 116001, <https://doi.org/10.1103/PhysRevD.65.116001>.
43. J. P. B. C. de Melo and T. Frederico, Light-Front projection of spin-1 electromagnetic current and zero-modes, *Phys. Lett. B* **708** (2012) 87, <https://doi.org/10.1016/j.physletb.2012.01.021>.
44. C. S. Mello *et al.*, Light-Front Spin-1 Model: Parameters Dependence, *Few Body Syst.* **56** (2015) 509, <https://doi.org/10.1007/s00601-015-0961-4>.
45. S. R. Amendolia *et al.*, A Measurement of the Pion Charge Radius, *Phys. Lett. B* **146** (1984) 116, [https://doi.org/10.1016/0370-2693\(84\)90655-5](https://doi.org/10.1016/0370-2693(84)90655-5).
46. S. R. Amendolia *et al.*, A Measurement of the Kaon Charge Radius, *Phys. Lett. B* **178** (1986) 435, [https://doi.org/10.1016/0370-2693\(86\)91407-3](https://doi.org/10.1016/0370-2693(86)91407-3).
47. R. Baldini *et al.*, Nucleon timelike form-factors below the N anti-N threshold, *Eur. Phys. J. C* **11** (1999) 709, <https://doi.org/10.1007/s100520050667>.
48. J. Volmer *et al.*, Measurement of the Charged Pion Electromagnetic Form-Factor, *Phys. Rev. Lett.* **86** (2001) 1713, <https://doi.org/10.1103/PhysRevLett.86.1713>.
49. H. P. Blok, G. M. Huber, and D. J. Mack, The Pion form-factor, In Exclusive Processes at High Momentum Transfer (2002) pp. 306-312.
50. T. Horn *et al.*, Determination of the Charged Pion Form Factor at  $Q^2 = 1.60$  and  $2.45$ -(GeV/c) $^2$ , *Phys. Rev. Lett.* **97** (2006) 192001, <https://doi.org/10.1103/PhysRevLett.97.192001>.
51. V. Tadevosyan *et al.*, Determination of the pion charge form-factor for  $Q^2 = 0.60$ -GeV $^2$  -  $1.60$ -GeV $^2$ , *Phys. Rev. C* **75** (2007) 055205, <https://doi.org/10.1103/PhysRevC.75.055205>.
52. C. D. Roberts, Electromagnetic pion form-factor and neutral pion decay width, *Nucl. Phys. A* **605** (1996) 475, [https://doi.org/10.1016/0375-9474\(96\)00174-1](https://doi.org/10.1016/0375-9474(96)00174-1).
53. F. T. Hawes and M. A. Pichowsky, Electromagnetic form-factors of light vector mesons, *Phys. Rev. C* **59** (1999) 1743, <https://doi.org/10.1103/PhysRevC.59.1743>.
54. P. Maris and P. C. Tandy, Electromagnetic transition form-factors of light mesons, *Phys. Rev. C* **65** (2002) 045211, <https://doi.org/10.1103/PhysRevC.65.045211>.
55. F. Carvalho *et al.*, Meson loop effects on the pion electromagnetic form-factor, *Phys. Rev. C* **69** (2004) 065202, <https://doi.org/10.1103/PhysRevC.69.065202>.
56. B. Desplanques, Nucleon and pion form-factors in different forms of relativistic quantum mechanics, *Int. J. Mod. Phys. A* **20** (2005) 1601, <https://doi.org/10.1142/S0217751X05023050>.
57. B. Desplanques, RQM description of the charge form factor of the pion and its asymptotic behavior, *Eur. Phys. J. A* **42** (2009) 219, <https://doi.org/10.1140/epja/i2009-10864-8>.

58. S. Noguera, Non local Lagrangians. (I): The Pion, *Int. J. Mod. Phys. E* **16** (2007) 97, <https://doi.org/10.1142/S021830130700565X>.
59. E. Santopinto, An Interacting quark-diquark model of baryons, *Phys. Rev. C* **72** (2005) 022201, <https://doi.org/10.1103/PhysRevC.72.022201>.
60. M. M. Giannini, E. Santopinto, and A. Vassallo, A New application of the Gursey and Radicati mass formula, *Eur. Phys. J. A* **25** (2005) 241, <https://doi.org/10.1140/epja/i2005-10113-4>.
61. E. Tomasi-Gustafsson and G. I. Gakh, Asymptotic behavior of nucleon electromagnetic form-factors in time-like region, *Eur. Phys. J. A* **26** (2005) 285, <https://doi.org/10.1140/epja/i2005-10164-5>.
62. E. Tomasi-Gustafsson *et al.*, Nucleon electromagnetic form-factors and polarization observables in space-like and time-like regions, *Eur. Phys. J. A* **24** (2005) 419, <https://doi.org/10.1140/epja/i2005-10030-6>.
63. V. A. Nesterenko and A. V. Radyushkin, Sum Rules and Pion Form-Factor in QCD, *Phys. Lett. B* **115** (1982) 410, [https://doi.org/10.1016/0370-2693\(82\)90528-7](https://doi.org/10.1016/0370-2693(82)90528-7).
64. L. X. Gutierrez-Guerrero *et al.*, Pion form factor from a contact interaction, *Phys. Rev. C* **81** (2010) 065202, <https://doi.org/10.1103/PhysRevC.81.065202>.
65. L. Chang *et al.*, Pion electromagnetic form factor at space-like momenta, *Phys. Rev. Lett.* **111** (2013) 141802, <https://doi.org/10.1103/PhysRevLett.111.141802>.
66. K. Raya *et al.*, Structure of the neutral pion and its electromagnetic transition form factor, *Phys. Rev. D* **93** (2016) 074017, <https://doi.org/10.1103/PhysRevD.93.074017>.
67. K. Raya, A. Bashir, and P. Roig, Contribution of neutral pseudoscalar mesons to aHLbL  $\mu$  within a Schwinger-Dyson equations approach to QCD, *Phys. Rev. D* **101** (2020) 074021, <https://doi.org/10.1103/PhysRevD.101.074021>.
68. S. Dalley, Impact parameter dependent quark distribution of the pion, *Phys. Lett. B* **570** (2003) 191, <https://doi.org/10.1016/j.physletb.2003.07.052>.
69. N. M. Kroll, T. D. Lee, and B. Zumino, Neutral Vector Mesons and the Hadronic Electromagnetic Current, *Phys. Rev.* **157** (1967) 1376, <https://doi.org/10.1103/PhysRev.157.1376>.
70. G. Krein, A. W. Thomas, and A. G. Williams, Charge symmetry breaking, rho - omega mixing, and the quark propagator, *Phys. Lett. B* **317** (1993) 293, [https://doi.org/10.1016/0370-2693\(93\)90998-w](https://doi.org/10.1016/0370-2693(93)90998-w).
71. H. L. L. Roberts *et al.*, pi- and rho-mesons, and their diquark partners, from a contact interaction, *Phys. Rev. C* **83** (2011) 065206, <https://doi.org/10.1103/PhysRevC.83.065206>.
72. T. Frederico and G. A. Miller, Null plane phenomenology for the pion decay constant and radius, *Phys. Rev. D* **45** (1992) 4207, <https://doi.org/10.1103/PhysRevD.45.4207>.
73. E. O. da Silva *et al.*, Pion and kaon elastic form factors in a refined light-front model, *Phys. Rev. C* **86** (2012) 038202, <https://doi.org/10.1103/PhysRevC.86.038202>.
74. J. P. B. C. de Melo *et al.*, Pairs in the light front and covariance, *Nucl. Phys. A* **631** (1998) 574C, [https://doi.org/10.1016/S0375-9474\(98\)00070-0](https://doi.org/10.1016/S0375-9474(98)00070-0).
75. P. Zyla *et al.*, Review of Particle Physics, *PTEP* **2020** (2020) 083C01, <https://doi.org/10.1093/ptep/ptaa104>.
76. J. J. Sakurai, Theory of strong interactions, *Annals Phys.* **11** (1960) 1, [https://doi.org/10.1016/0003-4916\(60\)90126-3](https://doi.org/10.1016/0003-4916(60)90126-3).
77. R. P. Feynman, Photon-hadron interactions, Editorial Addison Wesley Publishing Company, (1973).
78. J. P. B. C. de Melo *et al.*, The pion electromagnetic form-factor in a QCD-inspired model, *Few Body Syst.* **36** (2005) 189, <https://doi.org/10.1007/s00601-004-0099-2>.
79. G. P. Lepage and S. J. Brodsky, Exclusive Processes in Perturbative Quantum Chromodynamics, *Phys. Rev. D* **22** (1980) 2157, <https://doi.org/10.1103/PhysRevD.22.2157>.
80. G. R. Farrar and D. R. Jackson, The Pion Form-Factor, *Phys. Rev. Lett.* **43** (1979) 246, <https://doi.org/10.1103/PhysRevLett.43.246>.
81. A. V. Efremov and A. V. Radyushkin, Factorization and Asymptotical Behavior of Pion Form-Factor in QCD, *Phys. Lett. B* **94** (1980) 245, [https://doi.org/10.1016/0370-2693\(80\)90869-2](https://doi.org/10.1016/0370-2693(80)90869-2).
82. V. L. Chernyak, V. G. Serbo, and A. R. Zhitnitsky, Calculation of asymptotics of the Pion Electromagnetic Form Factor in the QCD Perturbative Theory, *Sov. J. Nucl. Phys.* **31** (1980) 552.
83. P. Maris and P. C. Tandy, The pi, K+, and K0 electromagnetic form-factors, *Phys. Rev. C* **62** (2000) 055204, <https://doi.org/10.1103/PhysRevC.62.055204>.
84. A. Faessler *et al.*, Pion and sigma meson properties in a relativistic quark model, *Physical Review D* **68** (2003), <https://doi.org/10.1103/physrevd.68.014011>.
85. D. Ebert, R. N. Faustov, and V. O. Galkin, Relativistic treatment of the decay constants of light and heavy mesons, *Phys. Lett. B* **635** (2006) 93, <https://doi.org/10.1016/j.physletb.2006.02.042>.
86. D. Ebert, R. N. Faustov, and V. O. Galkin, Masses and electroweak properties of light mesons in the relativistic quark model, *Eur. Phys. J. C* **47** (2006) 745, <https://doi.org/10.1140/epjc/s2006-02601-0>.
87. A. Bashir *et al.*, Collective perspective on advances in Dyson-Schwinger Equation QCD, *Commun. Theor. Phys.* **58** (2012) 79, <https://doi.org/10.1088/0253-6102/58/1/16>.
88. M. Chen and L. Chang, A pattern for the flavor dependent quark-antiquark interaction, *Chin. Phys. C* **43** (2019) 114103, <https://doi.org/10.1088/1674-1137/43/11/114103>.
89. P. T. P. Hutaeruk, I. C. Cloët, and A.W. Thomas, Flavor dependence of the pion and kaon form factors and parton distribution functions, *Phys. Rev. C* **94** (2016) 035201, <https://doi.org/10.1103/PhysRevC.94.035201>.

90. M. A. Ivanov *et al.*, Exclusive semileptonic decays of D and Ds mesons in the covariant confining quark model, *Front. Phys. (Beijing)* **14** (2019) 64401, <https://doi.org/10.1007/s11467-019-0908-1>.
91. S. Jia and J. P. Vary, Basis light front quantization for the charged light mesons with color singlet Nambu-Jona-Lasinio interactions, *Phys. Rev. C* **99** (2019) 035206, <https://doi.org/10.1103/PhysRevC.99.035206>.
92. P. Maris and C. D. Roberts, Pseudovector components of the pion,  $\pi^0$ – $\zeta$   $\gamma\gamma$ , and  $F(\pi)(q^{*2})$ , *Phys. Rev. C* **58** (1998) 3659, <https://doi.org/10.1103/PhysRevC.58.3659>.
93. G. Eichmann *et al.*, Single pseudoscalar meson pole and pion box contributions to the anomalous magnetic moment of the muon, *Physics Letters B* **797** (2019) 134855.
94. A. S. M. López, H. Sanchis-Alepuz, and R. Alkofer, Elucidating the effect of intermediate resonances in the quark interaction kernel on the time-like electromagnetic pion form factor, arXiv preprint arXiv:2102.12541 (2021)
95. C. A. Dominguez *et al.*, Pion form-factor in the Kroll-Lee-Zumino model, *Phys. Rev. D* **76** (2007) 095002, <https://doi.org/10.1103/PhysRevD.76.095002>.